

Time Domain Characteristics of Metal Magnetic/Eddy-current Sensor

Chun-Yeon Lin*, Yi-Chin Wu, Megan Teng, and Kuan-Cheng Chen

National Taiwan University, Taipei, Taiwan

*Corresponding author: chunyeonlin@ntu.edu.tw

Abstract: This paper presents a preliminary study on the design of the magnetic/eddy-current sensor to test plates made out of both ferrous and non-ferrous metals based on the time response analysis. Instead of the more prevalent double coil design, a compact anisotropic magneto-resistive sensor is used for the prototype of the magnetic/eddy-current sensor to detect the change in magnetic field density caused by the induced eddy-current on the test plates, lending more sensitivity to the sensing system. Several time-domain characteristics of the step response signal, including the time constant and steady-state value, are investigated. Numerical analysis from commercial finite element analysis software is conducted to display the variability of these characteristics, which shows promising results for characterizing three properties related to a metal plate: thickness, electrical conductivity, and magnetic permeability. Experiments are conducted to demonstrate the characteristics of time response corresponding to varying properties.

Keywords: Eddy-current Sensor; Electrical Conductivity; Magnetic Permeability; Time Response Analysis

1. Introduction

Eddy-current sensors are among one of the emerging fields of research for non-destructive sensing with its mechanical simplicity, long-term durability, and a wide range of applications, and within which a pulsed eddy current sensor uses either pulsed or step input signals to excite the coil instead of the conventional sinusoidal waves. Typical applications include crack detection [1], thickness classification of ferrous metal [2], and the thickness of the plating, such as the nickel coating of steel plates [3]. A shorter duration of the excitation frequency helps shorten the time needed for measuring, and with repetitive pulses, the sensor can be used to perform a continuous inspection on materials with local thickness variations or the structural integrity of larger objects such as an aircraft [4]. Compared to sweep frequency measurement, a pulse and the time response can be processed and analyzed more efficiently, and the hardware requirements are also less demanding. A short, precise energy burst also reduces the power consumption during the measurement, making it possible to be made into a portable device.

In this study, an anisotropic magneto-resistive (AMR) sensor is chosen to pick up changes in magnetic field density. A double coil design is often employed in most pulsed eddy current sensors, where the primary coil act as the excitation coil and the secondary as sensing coil, and the change in magnetic field density is perceived by measuring the change in the impedance of the sensing coil [5]. The Hall-effect sensor may also be deployed for the sensing of larger magnetic field intensity [6]. AMR sensor, on the other hand, has greater sensitivity than the options above, and the compact sizes of the sensor compared to a coil also allow the design to be made

portable. The placement of the sensor can also be more precisely orchestrated.

There are several ways to plan the input signal and interpret the output signal of a pulsed eddy-current sensor. The duration of the excitation pulse ranges from microseconds [7] to milliseconds, whereas some adopt a standard step input to observe both the rising of the signal and the steady-state behavior of the magnetic field [8]. Regarding the analysis of the response signal, previous work has been done on thickness measurement for ferrous metal using peak voltages of the time domain signals [9], and similar techniques could also be extended to the detection of material loss [3]. Some sensors require further signal processing. Further processing of the dataset, such as the Principle Component Analysis scores, is used to overcome the variability of the sensing environment [10]. Spectral analysis can also be conducted, such as using power spectral density analysis with wavelet transform to detect defects in aluminum plates [11]. Machine learning can also be implemented to improve the accuracy of thickness quantification of ferromagnetic materials [12].

Multiple factors with convoluted effects constitute the signal of the pulsed eddy-current sensor. For instance, the coupled effect of conductivity and permeability has to be separated by manipulating the shape of the excitation signal and the normalization [8]. Lift-off distance may also distort the measurement, and thus some studies have been done on sensors with immunity to lift-off distance [9, 13], and some choose to incorporate this measurement [14]. In this study, lift-off distance will be fixed by the design of the probe enclosure to eliminate its effect.

This paper offers a more comprehensive look into the

parametric effects of thickness, electrical conductivity, and the magnetic permeability of ferrous and non-ferrous metal plates on the time-domain responses of a step/pulse excitation signal. A preliminary classification of time-domain variations due to a specific parameter is discussed and identified to pave the way for further understandings of the sensor dynamics.

The remainder of this paper offers the following:

- 1) Numerical analysis is conducted to validate the parametric effects of permeability, conductivity, and thickness subjected to step input. Samples include both ferrous and non-ferrous metal plates. Characteristics of time response are examined to isolate features that could distinguish between different property values.
- 2) Experimental results are presented in accordance with the numerical analysis to offer a more empirical view of the effects illustrated above.

2. Metal Magnetic/Eddy-Current Sensor Design

Figure 1 illustrates the proposed Magnetic/eddy-current (M/EC) sensor design concept for characteristics of material properties for metallic objects. Fig. 1(a) shows that the M/EC sensor consists of an excitation coil and a one-dimensional anisotropic magnetoresistance (AMR) sensor. The AMR sensor measures the MFD generated from the ECDs induced in the metal plate with the step input current passing through the excitation coil. Under the assumption that the width of the plate is much larger than the M/EC sensor, the characteristics for the material and geometrical properties of the metal plate are electrical conductivity (σ), magnetic permeability (μ), and thickness (h).

Fig. 1(b) is the schematics of the M/EC sensor in the axisymmetric coordinate. (a_i, a_o, a) are the (inner radius, outer radius, half-length) of the excitation coil. The characteristics geometrical parameters of the M/EC sensor are normalized to a_o and a in dimensionless form with normalized coordinate ($R=r/a_o, Z=z/a$), EM ($\rho_i=a_i/a_o, \rho_o=a/a_o, D_w=d_w/a_o$), plate ($Z_p=z_p/a, H=h/a$), and sensor geometry ($Z_s=z_s/a$). D_w and N_E are the wire diameter and coil turns. Z_p, Z_s are the distances between the excitation coil and plate and sensor along the centerline. ($R_p=r_p/a_o$) is the radius of the plate. The time-varying currents (\mathbf{J}_E) passing through the excitation coil induce the Eddy-current on the metal. The excitation and the eddy-current induced in the metal contributed to the combined MFD measured at the AMR sensor. When the M/EC sensor operates in the air in the absence of a sample beneath, the perceived MFD in the air (\mathbf{B}_A) is equal to the sum of the MFD from the excitation (\mathbf{B}_E) and the environment (\mathbf{B}_G) in (1). Ideally, \mathbf{B}_A should be a pulse. On the other hand, in the case with samples beneath, the measured MFD consists of both \mathbf{B}_A and the one from the Eddy Current on the metal \mathbf{B}_M , which could be regarded as distributed current source.

The received MFD when the M/EC sensor is placed on the measuring object to perform measurements \mathbf{B}_C is contributed from the distributed current source is generated from \mathbf{B}_M , and \mathbf{B}_A in (2).

$$\mathbf{B}_A = \mathbf{B}_E + \mathbf{B}_G \quad (1)$$

$$\mathbf{B}_C = \mathbf{B}_A + \mathbf{B}_M \quad (2)$$

Fig. 1(c) illustrates the time response of the M/EC sensor with an input step current. The y-axis is the MFD normalized to the stationary MFD received in the air with the unit input current (B_0); the x-axis is the time.

τ and B_{ss} are the time constant and steady-state value of the measuring MFD when the M/EC sensor measures on the metal plate. The working principle of the M/EC sensor is to find the relationship between geometrical and material properties of the plate (σ, μ, h) and the features of the time response (B_{ss}, τ) so that the knowledge could be used to calculate the properties inversely.

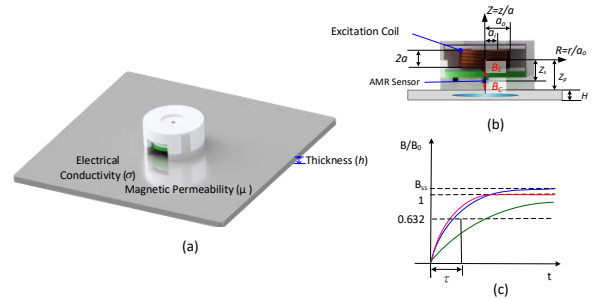


Fig. 1. Illustration of the time response analysis for the M/EC sensor design. (a) Hardware component. (b) Schematics showing parameters of the sensor. (c) Time response analysis.

A. Working Principles

Neglecting the effects of displacement current, the relationship between currents and electrical field can be formulated via Maxwell's equation that relates the magnetic and electric fields given by (3), (4) along with the constitutive relations in (5), (6). \mathbf{H} and \mathbf{E} are the magnetic and electrical field intensity. \mathbf{J} is the current density of the induced Eddy current both in the coil and metal, and \mathbf{B} denotes the magnetic flux density. σ, μ are electrical conductivity and magnetic permeability.

$$\nabla \times \mathbf{H} = \mathbf{J} \quad (3)$$

$$\nabla \times \mathbf{E} = -\frac{\partial \mathbf{B}}{\partial t} \quad (4)$$

$$\mathbf{B} = \mu \mathbf{H} \quad (5)$$

$$\mathbf{J} = \sigma \mathbf{E} \quad (6)$$

The magnetic flux density \mathbf{B} can be expressed as the the curl of magnetic vector potential (MVP) \mathbf{A} :

$$\mathbf{B} = \nabla \times \mathbf{A} \quad (7)$$

\mathbf{A} and \mathbf{B} have integral forms:

$$\frac{\mathbf{A}(\mathbf{r}, t)}{\mu_r} = \mathbf{A}_0(\mathbf{r}, t) = \frac{\mu_0}{4\pi} \int_{\Omega} \frac{\mathbf{J}(\mathbf{r}', t)}{|\mathbf{r} - \mathbf{r}'|} dV \quad (8a)$$

$$\mathbf{B}(\mathbf{r}, t) = \frac{\mu}{4\pi} \int_{\Omega} \frac{\mathbf{J}(\mathbf{r}', t) \times (\mathbf{r} - \mathbf{r}')}{|\mathbf{r} - \mathbf{r}'|^3} dV \quad (8b)$$

Where \mathbf{A}_0 is the MVP for non-ferrous metallic objects, μ_r is the relative magnetic permeability. Ω denotes the volume of the electric conductor. \mathbf{J} can be explicitly expressed in terms of \mathbf{A} by substituting \mathbf{B} from (7) into (4), leading to

$$\mathbf{E} = -\frac{\partial \mathbf{A}}{\partial t}. \quad (9)$$

Substituting (6) and (8a) into (9), the induced Eddy-current on the metal \mathbf{J}_M is expressed as a function of μ , σ :

$$\mathbf{J}_M = -\mu\sigma \frac{\partial \mathbf{A}_0}{\partial t}. \quad (10).$$

\mathbf{B}_M and \mathbf{B}_E are determined by substituting \mathbf{J}_M , \mathbf{J}_E into (8b).

B. Hardware Design

As shown in Figure 1(b), the sensor consists of one excitation coil and a one-dimensional AMR sensor to detect the z-component of MFD. The AMR sensor is more sensitive to slight deviations from the MFD and thus is particularly suitable for this kind of sensing method.

Fig. 2 shows the block diagram of the M/EC sensor. The input signal is generated by a personal computer (PC) and fed to the data acquisition system before being amplified by the power amplifier. The amplified signal then excites the coil and generates a change in magnetic flux density, inducing eddy current in the sample plate. The voltage across a power resistor in series with the coil can be measured to calculate the exact current that passes through it. The AMR sensor perceives the induced change in MFD and outputs a pair of differential voltage signals, which then pass through an instrumentation amplifier. PC then analyzes the time domain characteristics of the output signals from the AMR sensor.

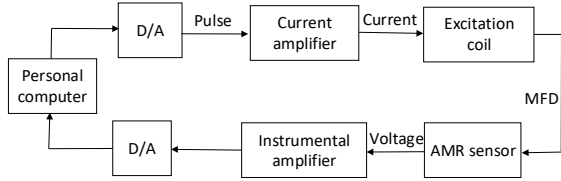


Fig. 2. Block diagram of the pulsed Eddy-current sensor.

3. Numerical Validation

The design and analysis of the proposed M/EC sensor are facilitated with commercial FEA software Comsol. The effect of electrical conductivity, thickness, and magnetic permeability on the time response analysis of time constant and steady-state value is validated.

Table 1. lists the parameters utilized in the simulation configuration of the excitation coil, AMR sensor, and sample plates. Four non-ferrous metals (Al, Cu, Mo, Zn) and two ferrous metals (Stainless steel, Ni) are used in the simulation. Non-ferrous metals have a constant μ_r of 1, while that of stainless steel lies within the range of 40 to 95, and for Nichrome, the range is 100-600. Fig.3 shows the schematics used in the simulation of Comsol.

Triangular elements and infinite boundary conditions are utilized in the simulation.

Table 1. Parametric Values of M/EC sensing System

System	
Excitation Coil	AMR Sensor (HMC1051ZL)
$N_w = 100$, $d_w = 0.35\text{mm}$	Size : $6.5 \times 1.7 \times 2.0$ mm
$(a_i, a_o, a) = (4.1, 7.2, 2.275)$ mm	$(r_s, z_s) = (0, 6.375)$ mm
Amplitude 1A, $t_w =$	Lift-off distance(z_p) = 9.225 mm
Plate ($r_p = 22.5$ mm)	
Non-Ferrous Metal ($\mu_r=1$)	
Aluminum (Al): $\sigma = 25.18$ MS/m	Copper (Cu): $\sigma = 58.85$ MS/m
Molybdenum (Mo): $\sigma = 18.1$ MS/m	Zinc (Zn): $\sigma = 16.48$ MS/m
Ferrous Metal	
Stainless steel	Nichrome (Ni):
$\sigma = 1.45$ MS/m	$\sigma = 0.67$ MS/m
$\mu_r=40-95$	$\mu_r=100-600$

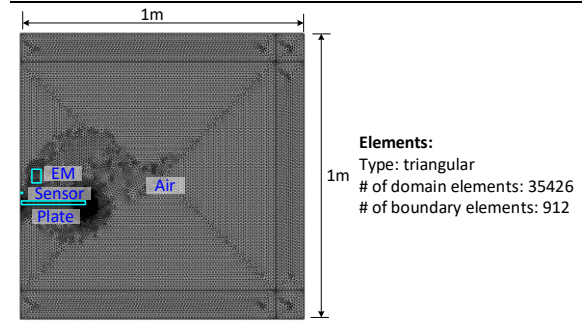


Fig. 3. Schematics illustrating parameters used in the simulation.

Fig. 4. shows the simulation results for the step responses of different scenarios. Fig. 4(a), (b) show the step responses for non-ferrous metals, but the same thickness plates (Al, Cu, Zn, Mo), and the Aluminum plates with different thicknesses, respectively. The simulation results show that changing the electrical conductivity and thickness of non-ferrous metal plates leads to different τ but same B_{ss} . Fig. 4(c), (d) show the step responses for ferrous metal plates (stainless steel and Ni) for different μ_r . The simulations results show that different μ_r leads to the same τ but different B_{ss} .

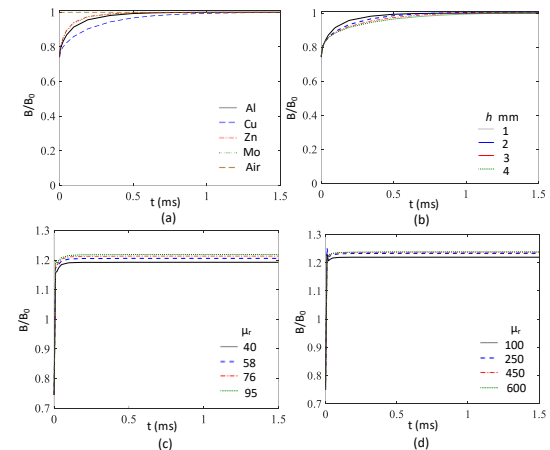


Fig. 4. Step response simulation results. (a) Same thickness, different non-ferrous metallic materials, and air. (b) Aluminum plate, different thickness. (c) Stainless steel, different magnetic permeability. (d) Nickel, different magnetic permeability.

Fig. 5(a) shows the relationship between the electrical conductivity, thickness, and time constant for non-ferrous metals. A linear relationship exists between electrical conductivity and time constant. Thickness vs. time constant can be curved fitted with a polynomial. Fig. 5(b) demonstrates the relationship between the magnetic permeability of ferrous metals and the steady-state value of the time response. The simulation results show that the magnetic permeability can be modeled as a second-order polynomial function of steady-state value regardless of the electrical conductivity.

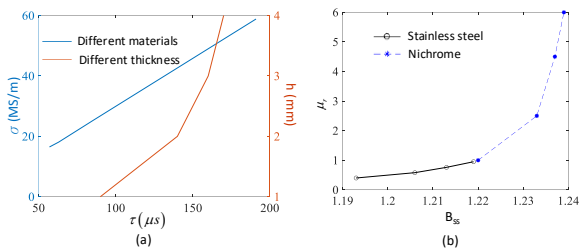


Fig. 5. Step response characteristics analysis. (a) different electrical conductivity, thickness vs. time constant for non-ferrous metals. (b) Magnetic permeability vs. time constant for ferrous metals.

4. Experimental Results

The experimental setup to investigate the time response analysis is shown in Fig. 6(a). The mechanical structure consists of a 3D-printed double-layered polylactic acid (PLA) case encapsulating the coil, an AMR sensor, and complementary circuits. Fig. 6(b) shows the probe made of an excitation coil and a commercial AMR sensor (HMC-1051ZL) beneath which are housed inside a PLA enclosure. An instrumentation amplifier is used to amplify the differential voltage signal from the AMR sensor. The PLA enclosure along with all the circuits and the probe itself, would be placed directly on top of the samples. The distance between the sensor and test samples is fixed to minimize interference and lift-off effect.

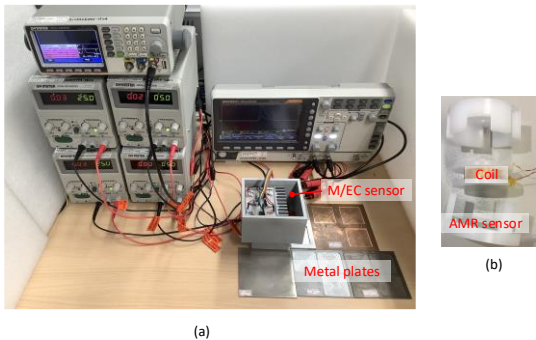


Fig. 6. M/EC sensing system. (a) Experimental setup (b) M/EC sensor.

Fig. 7 shows the experimental results. The y-axis is the MFD normalized to the MFD received in the air with unit input current (B_0); the x-axis is the time normalized to the input time width (t_w). As shown in Fig. 7(a), the input pulse of the excitation with 1.5 ms width and 5.1 μ s rise/fall time, and the signal obtained by the AMR sensor without metal plates placed below it. Fig. 7(b)-(d) are the time responses between metal plates of Ni and Cu (Fig. 7b), different non-ferrous metal plates (Fig. 7c), and different thicknesses of the aluminum plates (Fig. 7d). The experimental results show that magnetic permeability has a more significant impact on the time responses than electrical conductivity. The differences in thicknesses cause minor differences.

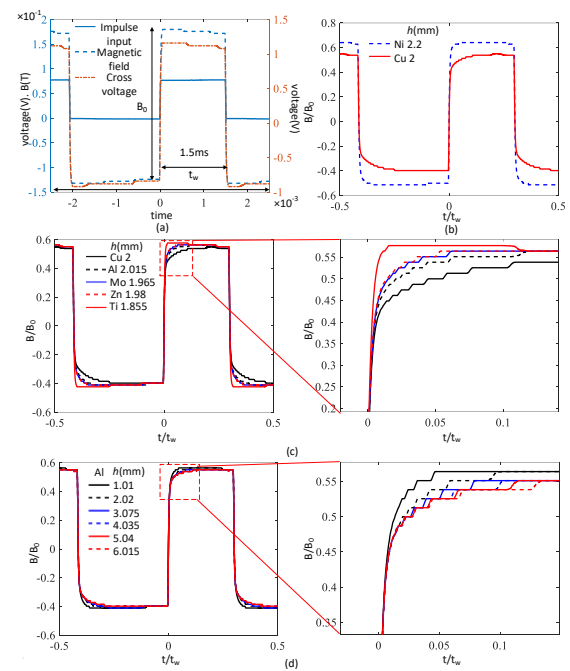


Fig. 7. Experimental results. (a) Input signal. (b) Metal plates. (c) Different non-ferrous metallic materials. (d) Different thicknesses of the aluminum plates.

Fig. (8a) shows the relationship between the electrical conductivity and rise time, fall time for non-ferrous metals. The difference in only electrical conductivity is inferred from the shape of the curve while fixing the geometry and magnetic permeability (all plates in the graph are non-ferrous). Such characteristics can be translated into a more qualitative analysis by examining the time constant of the rising and falling edge.

Plate thickness can also result in distinguishable disparities in the shape of the curve, as demonstrated in Fig. (7d), where only plate thickness varies across all test plates. The peak-to-peak voltage of the magnetic flux density pulse serves as a clue for thickness estimation, as displayed in Fig. (8b). It is also worth noting that the normalized peak values may vary depending on the material or the geometry of the test plates. However, a systematic classification of the implication of this observation requires further investigation.

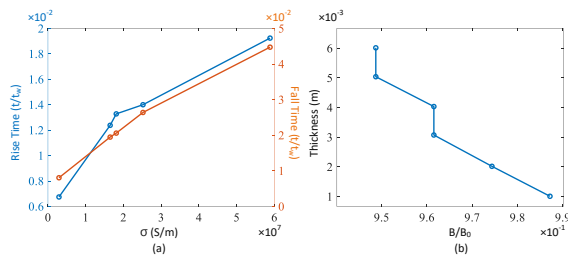


Fig. 8. Experimental results of pulse response characteristics analysis. (a) Different electrical conductivity vs. rise time, fall time for non-ferrous metals. (b) Different thicknesses of the aluminum plates.

5. Conclusion

Design and analysis of the M/EC sensor based on the time response analysis to characterize the metal objects have been presented. The link between time response from a step input and the properties of a metal plate is numerically validated. The simulation results show the viability to model electrical conductivity, thicknesses as a function of the time constant, and magnetic permeability as a function of steady-state responses. With a M/EC sensor prototype, the variations in time response on different metal materials and thicknesses have been illustrated experimentally. The features can be quantitatively characterized in future research for estimations of material and geometrical properties of different metals.

6. Acknowledgement

This work was supported by Ministry of Science and Technology, Taiwan, under Grant MOST 109-2628-E-002-005-MY3

7. References

- [1] Stott, C.A., et al., *IEEE Sensors Journal*, 15(2015) 956-962.
- [2] Park, D.G., et al., *IEEE Transactions on Magnetics*, 45(2009) 3893-3896.
- [3] Gotoh, Y., A. Matsuoka, and N. Takahashi, *IEEE Transactions on Magnetics*, 47(2011) 950-953.
- [4] Yang, G., et al., *IEEE Transactions on Magnetics*, 46(2010) 910-917.
- [5] Shu, L., et al., *Sensors and Actuators A: Physical*, 141(2008) 13-19.
- [6] Liu, Y., et al., *Journal of Nondestructive Evaluation*, 38(2018).
- [7] James, H.R., U. Erol, and C.M. John., *Proc.SPIE.* (1994).
- [8] Adewale, I.D. and G.Y. Tian, *IEEE Transactions on Magnetics*, 49(2013) 1119-1127.
- [9] Wang, H., W. Li, and Z. Feng, *IEEE Transactions on Instrumentation and Measurement*, 64(2015) 2557-2564.
- [10] Horan, P.F., P.R. Underhill, and T.W. Krause, *IEEE Sensors Journal*, 14(2014) 171-177.
- [11] Qiu, X.B., et al., *IEEE Transactions on Magnetics*, 50(2014) 1-8.

[12] Ulapane, N., et al., *IEEE Sensors Journal*, 21(2021) 5413-5422.

[13] Yin, W. and K. Xu, *IEEE Transactions on Instrumentation and Measurement*, 65(2016)164-169.

[14] Meng, X., et al., *IEEE Transactions on Instrumentation and Measurement*, 70(2021) 1-8.